ELSEVIER

Contents lists available at ScienceDirect

# **Applied Surface Science**

journal homepage: www.elsevier.com/locate/apsusc



# Full length article

# GaAs layer on c-plane sapphire for light emitting sources

Rahul Kumar<sup>a,\*</sup>, Samir K. Saha<sup>b</sup>, Andrian Kuchuk<sup>c</sup>, Yurii Maidaniuk<sup>c</sup>, Fernando Maia de Oliveira<sup>c</sup>, Qigeng Yan<sup>b</sup>, Mourad Benamara<sup>c</sup>, Yuriy I. Mazur<sup>c</sup>, Shui-Qing Yu<sup>c,d</sup>, Gregory J. Salamo<sup>b,c</sup>

- <sup>a</sup> Department of Electrical and Electronics Engineering, Birla Institute of Technology and Science, Pilani, Pilani 333031, India
- <sup>b</sup> Department of Physics, University of Arkansas, Fayetteville, AR 72701, USA
- <sup>c</sup> Institute for Nanoscience and Engineering, University of Arkansas, Fayetteville, AR 72701, USA
- <sup>d</sup> Department of Electrical Engineering, University of Arkansas, Fayetteville, AR 72701, USA

#### ARTICLE INFO

# Keywords: Dissimilar Epitaxy Microwave photonics Twinning Quantum well Two-step growth MBE

#### ABSTRACT

High-quality cubic GaAs (111)A buffer layers have been grown on an atomically flat c-plane trigonal sapphire substrate having well-defined steps and terraces. A two-step growth method has been used where, at an early stage, a GaAs layer has been grown at low temperature (LT), followed by second high-temperature GaAs growth layer. In addition to the two-step growth process, an AlAs nucleation layer and multiple annealing steps have been employed. The effectiveness of the LT GaAs layer in this highly dissimilar epitaxy was then investigated. An LT GaAs layer resulted in a relaxed GaAs buffer with smooth surface morphology and high crystalline quality. An InGaAs quantum well (QW) was epitaxially grown on the 70 nm GaAs buffer and compared with a reference InGaAs QW grown on a GaAs (111)A substrate. Along with x-ray and high-resolution cross-section transmission electron microscopy, comparable QW photoluminescence intensity and linewidth with respect to reference InGaAs QW confirmed the effectiveness of our growth strategies to produce high-quality GaAs on sapphire. This demonstrates the opportunity for GaAs photonics on sapphire and the potential to realise an integrated microwave photonic chip on a sapphire platform.

## 1. Introduction

As a result of the fact that GaAs is a direct band gap semiconductor, it has found many light-emitting applications. In fact, with applications in mind, GaAs has been grown on both native and foreign substrates for decades. Most of these reports have used substrates having a similar cubic crystal structure [1,2]. In this paper, we report on ultrathin cubic GaAs buffers (60–70 nm) having high crystal quality that has been grown on a dissimilar substrate - trigonal c-plane sapphire.

The reason for choosing sapphire is that it is an ideal platform for integrated microwave photonics (IMWP). As a substrate, sapphire has the immediate advantage of an existing silicon on sapphire (SOS) technology for electronics components and an existing body of work on  $\mathrm{Si}_3\mathrm{N}_4$  on sapphire for waveguide and passive components. It also has the very important advantages over other substrates, such as silicon, of an excellent coefficient of thermal expansion match with III-V semiconductors. As a result, enabling the growth of an efficient light-emitting material, such as III-V semiconductors on sapphire, can be significant to

the realization of complete integration of MWP functionality on a single photonic chip. In addition, the GaAs on sapphire system has other important material properties, such as a large refractive index contrast between GaAs and sapphire; a high resistivity of the sapphire substrate; transparency of the sapphire substrate near the III-As band gap providing the potential for 3D photonic systems [3,4]; and importantly, at low cost. These properties make GaAs on sapphire an ideal system for IMWP and more generally, photonic applications.

However, the realization of this ideal platform comes with great challenges. Two of these challenges are (i) the large lattice constant mismatch and (ii) dissimilar crystal structure between GaAs and sapphire. Atomic arrangements of the c-plane of sapphire and GaAs (111) plane are shown in Fig. 1. The lattice mismatch is  $\sim\!46\%$  compressive if we assume there is a one-to-one mapping between Ga/As atoms in GaAs to oxygen atoms in sapphire. The lattice mismatch is  $\sim\!16\%$  tensile if we assume there is a one-to-one mapping between Ga/As atoms in GaAs to octahedral hollows in sapphire. In spite of the ever-increasing expansion of the sapphire substrate in different fields of electronics and

E-mail address: rkp203@gmail.com (R. Kumar).

<sup>\*</sup> Corresponding author.

optoelectronics [5], the cubic III-V on sapphire system has been almost untouched except with few scattered reports [6–11]. However, our initial research on this system has encouraged to investigate its potential for IMWP [4].

When grown on c-plane sapphire, GaAs selects a (111)A orientation. The result is a rough surface with 60° rotated twin defects which are common even for homoepitaxially grown GaAs (111)A [12]. In addition, the large lattice mismatch and interface energy result in the generation of misfit and threading dislocations in the epitaxial layer. Managing dislocations to achieve a high-quality GaAs active layer is, therefore, a serious challenge. More generally, in previous studies on reducing the level of dislocation defects, a buffer layer is commonly used to confine generated dislocations and to produce a template for further growth of active layers having a significantly lower dislocation density [13,14]. The desirable evolving properties of the buffer are: (a) fully relaxed, (b) smooth surface, and (c) low threading dislocation density [15]. To achieve these properties, a two-step growth technique has been used successfully [16–21]. This paper utilizes a similar low temperature (LT) GaAs layer as a first step, followed by a higher temperature (HT) growth layer, to suppress threading dislocations (TDs) and produce an ultrathin GaAs buffer, which provides a highly relaxed, smooth active surface that produces high-quality photoluminescence.

There are different models in the literature offered to explain the mechanism by which an LT GaAs buffer significantly reduces the dislocation density. Of these, the most common model is based on "dislocation bending" at the LT GaAs/HT GaAs interface due to the sudden transition in stress. At the interface, the lattice constant of GaAs grown at LT is larger than the lattice constant that forms at HT GaAs due to arsenic "antisite defects" [16,17,21]. As a result, there is a lattice mismatch at the LT GaAs/HT GaAs interface that produces misfit dislocations which, in turn, suppress the threading dislocations by bending. Other models are based on dislocation blocking during island coalescence [22] or an introduction of dislocations model, that happens before or after island coalescence [23]. In any case, a two-step LT GaAs/HT GaAs approach has been taken in the research reported in this paper. More specifically, the schematic of the structures investigated, with a total growth time of about 1 h, is shown in Fig. 2(a). A thin AlAs layer (5 nm) has been grown before the GaAs layer. This improves the wetting of the substrate, reduces twinning, and enhances the quality of the GaAs, as reported in our earlier publication [4]. More specifically, multiple annealing growth interruptions was found to achieve twin-free GaAs [4].

In this research, we investigated, the importance of the thickness of

the LT-GaAs layer (which depends on the growth time " $t_1$  mins" in Fig. 2 (a)) on the quality of the GaAs buffer grown on c-plane sapphire. The XRD, surface smoothness and PL were studied as a function of the thickness of the LT layer. Finally, an InGaAs quantum well was grown on the GaAs buffer (shown in Fig. 2(b)) and compared with an InGaAs quantum well (QW) grown on a GaAs (111)A substrate with a GaAs buffer as a test of the quality of the buffer and the quantum well.

# 2. Experimental procedure

All samples were grown by solid source molecular beam epitaxy (MBE). Substrates were backside coated with 1 µm titanium for uniform and efficient heating. Before transferring to the load lock chamber, substrates were degreased with acetone, methanol and deionized (DI) water. In the load lock chamber, they were heated at 200 °C for 1 h to mainly evaporate any water remaining from the cleaning process. Afterward, substrates were transferred to the degassing chamber where they were annealed at 900 °C for 6 h and then transferred to the growth chamber. In the growth chamber, substrates were heated to 900  $^{\circ}\text{C}$  for 3 h to get a clean smooth surface free of any organic contaminants. Before starting the growth, we exposed the surface to an arsenic flux of 5  $\times$ 10<sup>-6</sup> Torr at 650 °C for half an hour [9]. The substrate was then heated to the growth temperature according to the thermocouple reading. However, the actual surface temperature of the substrates maybe 30 to 100 °C less than the thermocouple temperature since the thermocouple is not touching the surface of the substrate. The growth rates of GaAs and AlAs were 0.75 ML/s and 0.2 ML/s, respectively. These growth rates were calibrated on GaAs (100) substrates where sticking coefficients of Ga and Al are close to unity. The V/III beam equivalent pressure (BEP) ratio during GaAs growth was 40. During the growth, real-time monitoring was done using reflection high energy electron diffraction (RHEED) set at 20 keV accelerating voltage and 1.5 A cathode current at a glancing angle of  $1-2^{\circ}$  to the substrate.

The surface morphology of each sample was investigated by atomic force microscopy (AFM) (Bruker, model number 3000 dimension III) using the tapping mode. AFM was performed using stable, sharp tips (Si tip material, tip radius  $\sim 10$  nm) with optimized feedback and force parameters. To measure the optical properties, samples were mounted in a closed-cycle cryostat (Janis CCS-150) for the low-temperature photoluminescence (PL) measurements at 10 K. A 532-nm continuous-wave laser was used to optically excite the sample and a liquid nitrogencooled CCD detector array (Princeton Instruments PyLoN: 1024-1-.7) attached to a 50-cm focal-length spectrometer (Acton 2500) was used

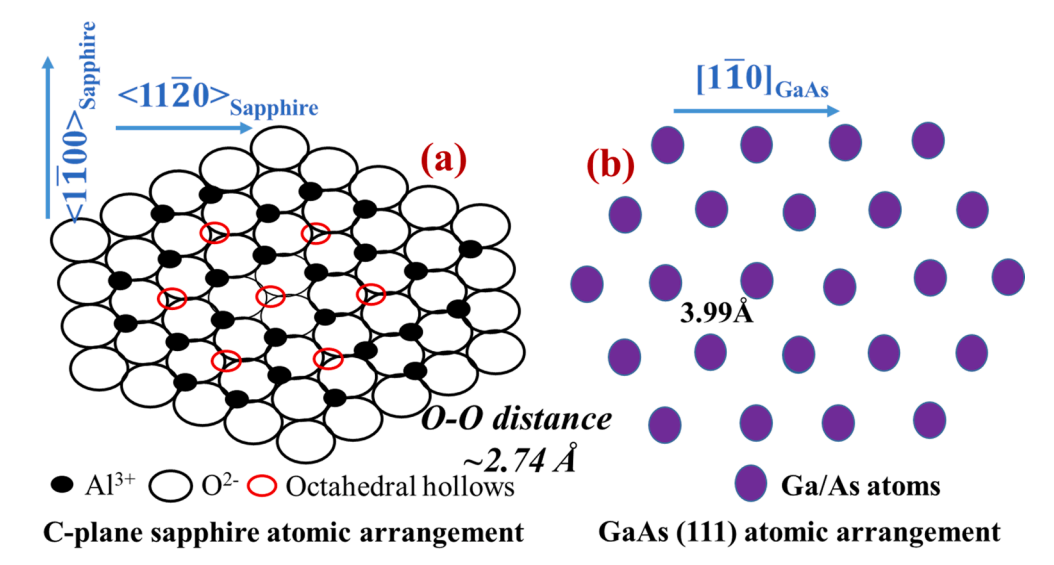


Fig. 1. (a) C-plane sapphire atomic arrangement showing one layer of oxygen atoms and one layer of Aluminum atoms, (b) either Ga or As atomic plane for GaAs (111).

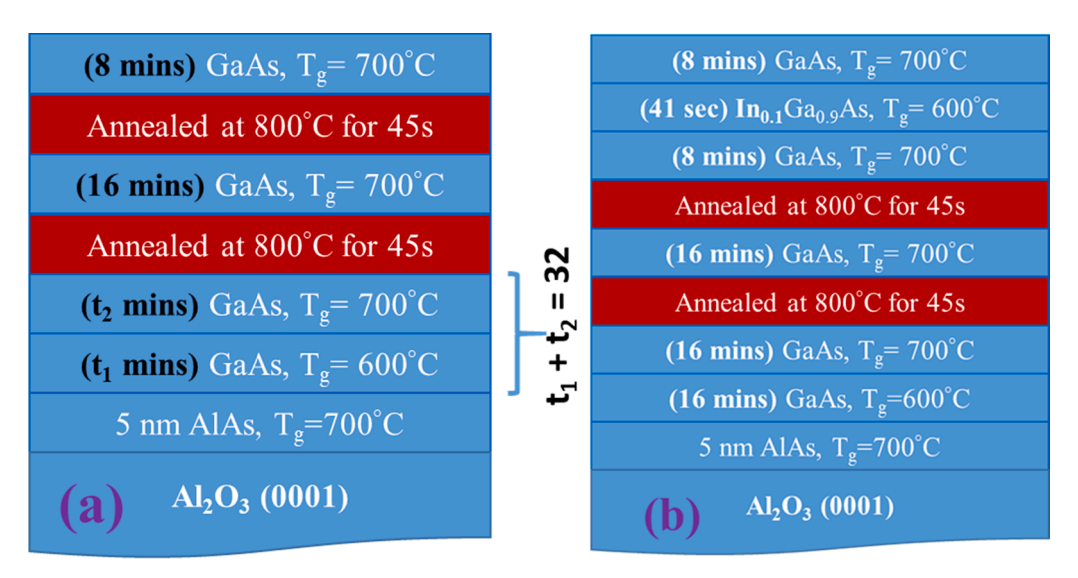


Fig. 2. (a) Generalized schematic structure of samples presented in this work; (b) schematic structure of InGaAs QW.

to detect and investigate the PL signal. To understand the structural properties and crystalline quality of grown materials, a PANalytical X'Pert MRD diffractometer equipped with a multilayer focusing mirror, a standard four-bounce Ge (220) monochromator providing a collimated and monochromatic incident Cu Ka1 source of radiation ( $\lambda=0.15406$  nm), and a Pixel detector, was used for the x-ray diffraction (XRD) scans. To evaluate the strain in the GaAs buffer, micro-Raman measurements were conducted at room temperature using a Horiba LabRAM HR800 system equipped with a He—Ne laser ( $\lambda=633$  nm, power = 5 mW), a 0.75 m spectrometer, and a thermoelectrically cooled Si charge-coupled device (CCD). An Olympus BX41 microscope equipped with a  $100\times$  objective was used to focus the laser light on the sample to a spot size of about 1  $\mu$ m and collect the backscattered Raman signal. An edge filter was placed in the collected light to remove the elastically scattered laser light at 633 nm.

To determine the semiconductor film thickness, spectroscopic ellipsometry (WVASE32), with the capability to measure at different angles of incidence (65°, 70° and 75°) and having a resolution of 10 nm, was used to collect spectroscopic data in the range of 0.496–4.768 eV (260–2500 nm). A built-in WVASE32® software was used to perform the data fitting process. Meanwhile, to investigate interfaces, a transmission electron microscope (TEM) was used. In this case, the sample was polished until 20  $\mu m$  thickness using an Allied High Tech Products Inc. polisher. A Fischione 1010 low-angle ion milling instrument was used to make the needed hole in the center of the sample. Using a Cs corrected

Titan 80-300, with a Schottky field emission gun (FEG) that is operated at 300 kV, cross-sectional high-resolution TEM (HRTEM) images were taken. A TF20 TEM, with electron sources operated at 200 keV, was also used

#### 3. Results and discussion

# 3.1. Surface characterization

All sapphire substrates, used in this research, possess a well-defined step-terrace surface. The importance of having a step-terrace and clean substrate surface for dissimilar material growth is shown in earlier publications [4,24]. This surface was achieved by heating as-received substrates at 1200 °C for 6 h in atmospheric conditions. Fig. 3 shows the representative AFM images of an as-received substrate and a well-defined step terrace surface. After annealing, the substrate surface is atomically flat and clean. The surface has terrace heights of 1 monolayer (0.2–0.3 nm) and terrace widths around 200–300 nm. The unintentional miscut of substrates used was less than 0.1°, as calculated from Fig. 3(b). A line profile of the surface along the perpendicular direction of steps is shown in the top right inset of Fig. 3(b), where one monolayer high step can be easily seen. Bottom right inset of Fig. 3(b) shows the RHEED from the sapphire substrate just before the growth. Narrow streaks and Kikuchi lines validate the cleanliness of the prepared substrate.

To study the effectiveness of the added growth of an LT GaAs layer,

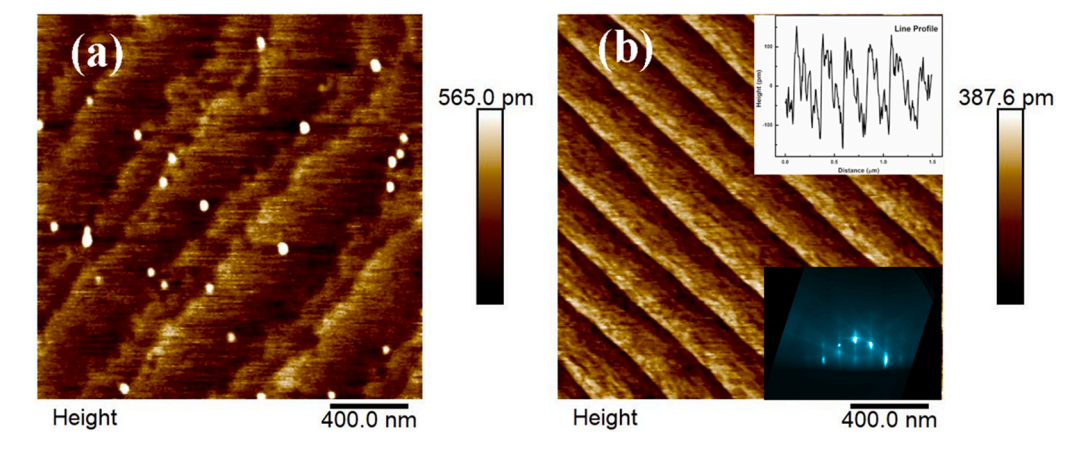


Fig. 3. AFM image of (a) as received sapphire substrate (b) surface after annealing. The top-right inset shows the line profile perpendicular to the surface steps and the bottom-right inset shows the RHEED along [1120] of sapphire from the cleaned substrate just before the growth.

three different samples are grown with different thicknesses LT layer corresponding to the growth time of 16 min (S1), 8 min (S2) and 0 min (S3). The growth temperature of GaAs layers after the LT GaAs layer is 700 °C. AFM surface morphology of these samples is shown in Fig. 4 (a-c). Pyramidal hillocks are observed on the surface of all samples. Random shaped large and deep pits are observed on the sample without an LT layer (S3). Most of these pits have penetrated up to 60 nm of GaAs film. Fig. 4(d) and (e) show the RHEED after the growth of these samples. For the sample with no LT GaAs growth or  $t_1 = 0$  (S3), a streaky RHEED pattern is observed, with clear spots on the streaks. Meanwhile, for samples grown with an LT GaAs layer (S1 and S2), the observed streaky RHEED pattern is (2  $\times$  2) indicating smoother surface morphology of S1 and S2 after growth compared to the rougher surface for S3. The root mean square (RMS) surface roughness on the scan area of 5  $\mu$ m  $\times$  5  $\mu$ m, observed for samples S1, S2 and S3 are 1.76 nm, 1.55 nm, and 9.46 nm, respectively. Both RHEED and AFM confirm that the presence of an LT layer results in smoother surface morphology of the GaAs layer. Even though the RMS roughness value of S1 is higher than S2, the pyramidal hillock density is smallest in S1. The appearance of pyramidal surface features is very common for GaAs growth on a GaAs (111)A surface and has been explained either by a high Ehrlich-Schwöbel (ES) barrier [12] or by adatom motion in presence of stacking faults [25,26]. However, growth on the homoepitaxial GaAs (111)A surface does not show surface pits. Pit formation then likely has a different origin. For GaAs (111) surfaces, the formation of etch pits have been reported after thermal and chemical treatment [27,28]. It is generally accepted that these etch pits are related to defects in the crystalline film [28-30]. Presence of pits on the surface of S3 is indicative of high defect density in the film during growth and subsequent pit formation by etching during the growth and/or annealing processes. For example, etching could be the result of Ga droplet formation during growth, considering the lower sticking coefficient of arsenic on a GaAs (111)A surface.

Results obtained from XRD and ellipsometry show that the thickness of GaAs film is around 70 nm, far from the nominal thickness we expected. Thickness values for all three samples are listed in Table 1. The lower actual thickness of the GaAs film compared to the nominal thickness values can be understood by recognizing the very low sticking coefficient of As on GaAs (111)A surface compared to the GaAs (001)

**Table 1** Thickness of III-As film on sapphire.

Measurement method	S1	S2	S3
XRD	71 nm	72 nm	NA
Ellipsometry	61 nm	69 nm	62 nm

surface [31]. The depth of the pits in S3 is almost the same as the thickness of the GaAs. It is highly possible that the observed pits in the AFM image of S3 have penetrated down to the thin AlAs nucleation layer. This could happen either because of a lower growth rate on top of the defected region in AlAs and/or due to the evaporation of material during annealing from the defected region.

#### 3.2. Structural characterization

From symmetric  $\omega$ -20 scans of all three samples, shown in Fig. 5(a, b), only (111) crystal orientation was observed. It is very important to notice in Fig. 5(a) that the interference fringes can be observed in the two samples with the LT layer (S1 and S2) and no fringes are observed in the sample without an LT layer (S3). Absence of interference fringes is mainly related to the non-uniform thickness of GaAs film due to the rougher surface morphology of the sample S3. The fringes were very prominent for sample S1 than the sample S2 although the RMS roughness of S1 is higher than S2. This could be because the surface of S1 has a larger area of high smoothness. Importantly, observed fringes correspond to the total GaAs thickness of 72  $\pm$  5 nm (both in the case of S1 and S2), listed in Table 1.

Fig. 5(b) shows the peak shift of the GaAs (111) peak with respect to sapphire (00.6) peak. Samples show the shift in peak from the bulk GaAs peak position. Either strain or crystallographic tilt in an epitaxial film can cause the shift in the peak position [14,32]. Hence, it's difficult to conclusively state the strain in GaAs film from these  $\omega$ -20 scans. Raman spectroscopy is a great tool to measure the strain in thin films. Fig. 5(c) shows the Raman spectroscopy of three samples along with GaAs (111)A substrate. Raman shifts of GaAs longitudinal optical (LO) peak for S1 and GaAs substrate are almost same. Sample S3 shows the lowest phonon frequency for GaAs LO peak and the highest strain among the three samples. These results suggest that S1 has the least strain whereas

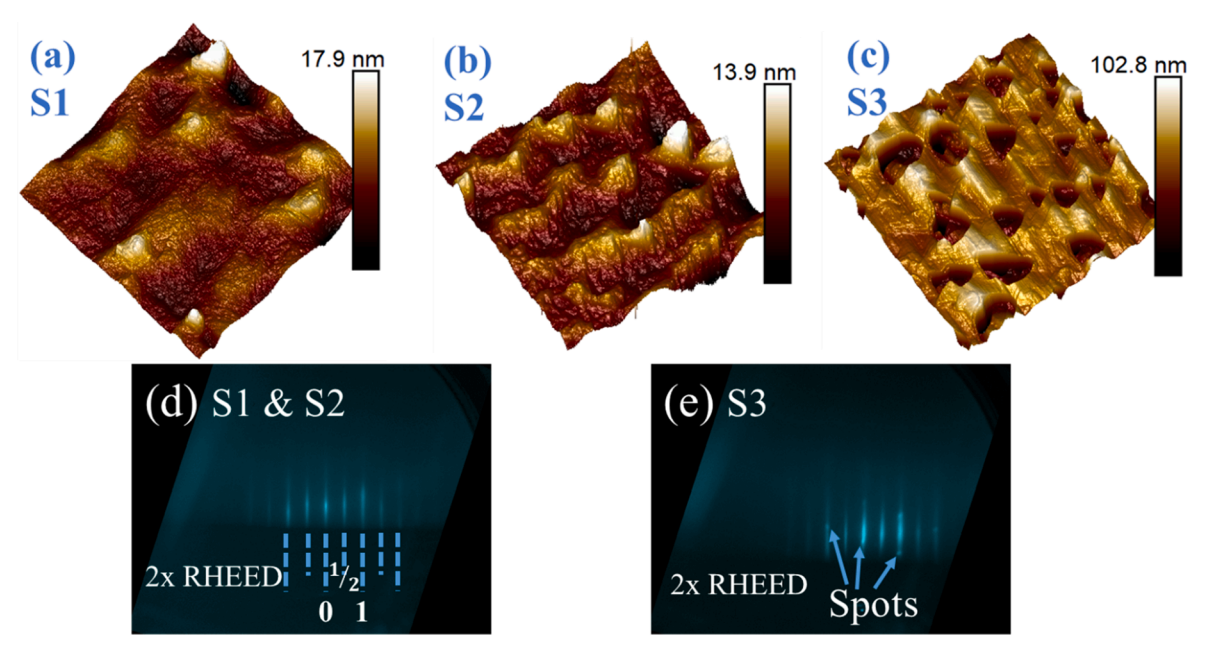


Fig. 4. AFM images ( $5 \mu m \times 5 \mu m$ ) of (a) S1, (b) S2, (c) S3; RHEED images along [ $1\overline{1}0$ ] direction of GaAs (d) after growth of entire structure of S1 and S2, 0th, ½th and 1st order RHEED streaks are marked, longer broken lines show the integer-order RHEED streaks whereas shorter broken lines show fractional-order RHEED streaks; and (e) after growth of S3, spots riding on streaks can be seen, few spots are shown by arrows.

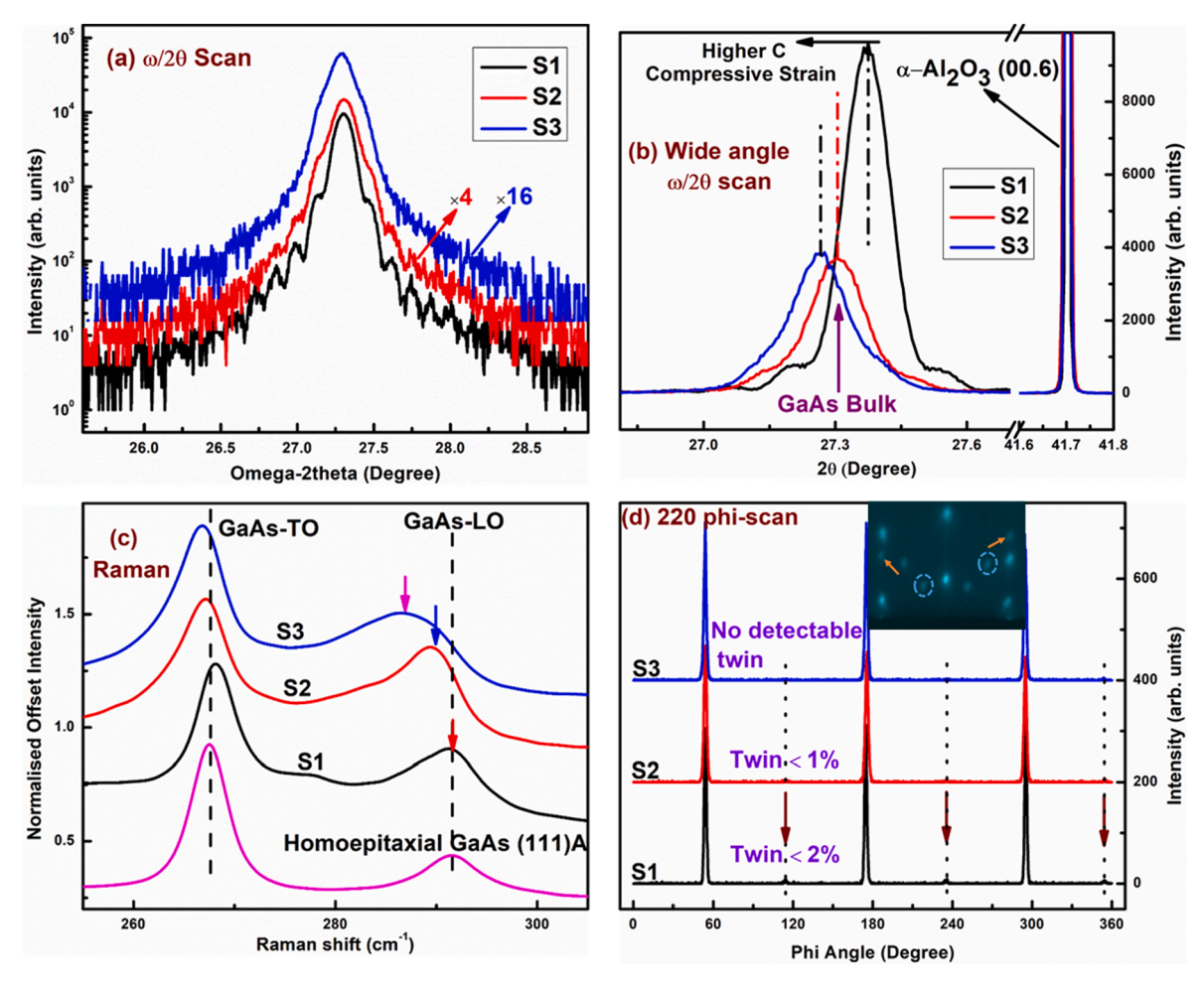


Fig. 5. (a) Omega/2theta scan of samples grown with three different LT layer thickness', GaAs peak is centered at same  $2\theta$  angle to show the shape variation and fringes of GaAs (111) plane diffraction peak in three samples; (b) (111) symmetric Omega/2theta scan showing the shift of GaAs (111) peak with respect to sapphire (00.6) peak; (c) Raman spectra of these samples with homoepitaxial GaAs (111)A sample, arrows pointing the GaAs longitudinal optical (LO) phonon peaks of these three samples show the gradual shift of LO peak from homoepitaxial GaAs, TO stands for transverse optical phonon peak; and (d) phi-scan of (220) plane for these three samples showing the twinning in GaAs film, dotted line show the peak position for  $60^{\circ}$  twins, Arrows show the peak positions of (10.4) planes of sapphire, the Inset shows the representative RHEED along [1 $\overline{10}$ ] direction after LT GaAs growth in S1 and S2, some spots corresponding to rotational twins have been shown by arrows while spots corresponding to reflection twins have been shown by dashed circles.

S3 is the most tensile strained among all thee samples.

Phi-scans for the (220) plane of GaAs has been plotted in Fig. 5(d) where arrows show the (10.4) planes of sapphire substrate. Equally separated three (10.4) planes show the trigonal space symmetry of sapphire substrate. From the phi-scan (and also from RHEED), In-plane epitaxial relation between the sapphire substrate and GaAs is found to be  $\left[11\overline{2}0\right]_{Sapphire} \parallel \left[1\overline{1}0\right]_{GaAs}$ . Phi-scans for each of these three samples show almost no twinning. A slight hump does appear in phi-scan for S1. This can be explained as due to the low growth temperature, a large amount of twins are generated early in this stage, which can be seen in the RHEED image after LT GaAs growth (shown in the inset of Fig. 5(d)). A rough surface and the presence of twinning are observed in the RHEED pattern. However, superior PL and rocking curve (RC) linewidth (will be shown in later sections) indicate that these twins do not penetrate to top GaAs layers. This also confirms the effectiveness of the annealing steps to suppress twins.

Fig. 6(a) shows the HRTEM image of sample S1 near the interface. A sharp film/substrate interface can be seen indicating the high quality of sapphire substrate. As expected, the film/substrate interface is highly defective. A stacking fault (SF) is shown in the image by a broken line. Even though the material near the film/substrate interface is defective, these defects are mostly confined and do not propagate to the top GaAs

layer. As a result, good quality GaAs is obtained after only 70 nm of growth. It demonstrates the high effectiveness of the LT GaAs layer to confine defects within itself. Fig. 6(c) shows the effect of defect propagation to the surface of the film to cause a pit at the surface.

The rocking curves (RCs) of these three samples are shown in Fig. 6 (b). The RC measurement or omega scan is an effective way to assess the crystalline quality of the material. More specifically, the higher the linewidth of the RC the lower the crystal quality. RCs of all three samples show a sharp peak with broadening at the base of the curves, suggesting that the curve is the sum of two effects. Each RC is fitted with two Gaussian curves: one with a lower linewidth and the other with the higher linewidth. Table 2 listed the results of Gaussian fittings of these three samples. The sample with no LT layer (S3) shows the highest ratio of integrated intensity between the broader and sharper peaks while sample S1 shows the lowest value of this ratio. One possible explanation for this RC base broadening is the presence of point defects in GaAs. A diffuse scattering peak is often observed in epitaxial layers and is associated with the presence of point defects [33]. A second possible explanation is that these two curves can arise from two different regions of different quality GaAs that make-up the film. We have seen the HRTEM result indicating that the region closer to the film-substrate interface has poorer quality than the region away from the interface. In S3, the higher integrated area of the broader peak with respect to the

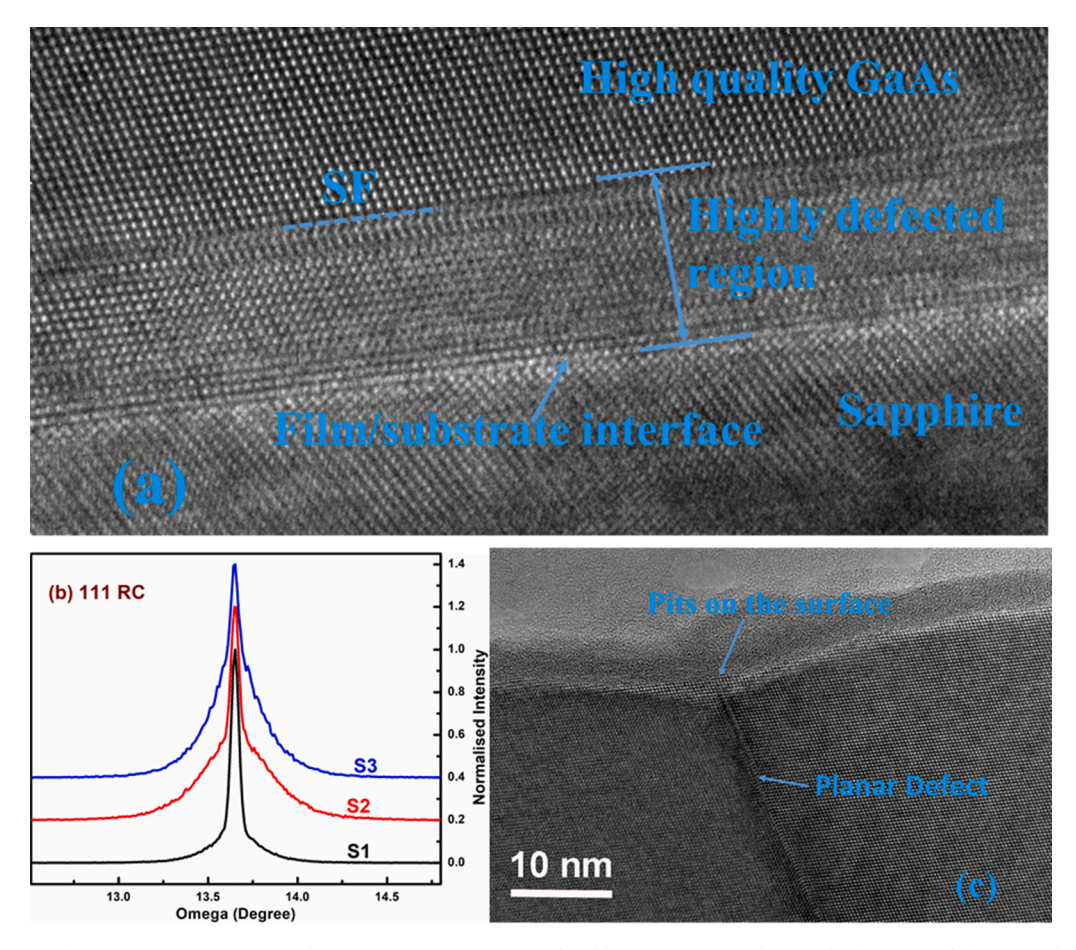


Fig. 6. (a) Cross-sectional HRTEM image of S1 near film/substrate interface, SF is the abbreviation for stacking fault; (b) RC of all three samples (c) HRTEM image showing the formation of a pit on the surface due to extended defect.

**Table 2**Linewidth and integrated intensity ratio of broader and sharper curves from Gaussian fitting of RC for samples S1, S2, and S3.

Sample ID	Linewidth of sharper peak (arcsec)	Linewidth of broader peak (arcsec)	Integrated intensity ratio of broader to sharper peak
S1	187.2	1195	1
S2	187.2	1710	5.2
S3	212.4	1364	6.6

sharper peak indicates that this sample has either a higher volume of low-quality GaAs or simply has more point defects. Either way, RC indicates that the presence of the LT layer improves the crystalline quality of GaAs. Judging from HRTEM, the higher quality of GaAs in S1 might be related to efficient bending of dislocations along the LT GaAs/GaAs interface to form misfit dislocations (MDs). This is reasonable since there is higher stress accumulation at the interface due to the higher thickness of the LT layer in S1.

## 3.3. Photoluminescence (PL)

We also investigated the photoluminescence from the three samples which are shown in Fig. 7(a). S1 shows the highest PL peak intensity among the three samples. This is consistent with the highest GaAs layer quality as indicated by the XRD and AFM results. Noticeably, the GaAs PL peak does not occur at the same energy for all three samples. Probably, this is because of the effect of background noise, especially in the case of S3.

In summary, the narrower PL and RC linewidths along with a higher

PL intensity of S1 indicate that it has less defect density near the top GaAs layer and it would be the best candidate among the three as a template to grow active device layers on it. With this in mind, we grew a 10 nm wide  $In_{0.1}Ga_{0.9}As/GaAs$  QW (S1-QW) on top of S1. The composition and thickness values of the QW are nominal. We also grew the same QW on a GaAs (111)A substrate (p-InGaAs-QW). The PL spectra of QW samples are shown in Fig. 7(b). Theoretical PL peak position for electron energy level to heavy-hole energy level is near 1.37 eV. However, the observed PL transition energy of QW is 1.49 eV. We have already seen the small actual thickness of the GaAs compared to the nominal thickness, likely due to the different sticking coefficient. The PL linewidth, peak position and integrated intensity of the QW peak from both samples are listed in Table 3. The PL intensity of the InGaAs QW on sapphire is of the same order as observed for the QW on the GaAs substrate. Moreover, the integrated intensity of the QW peak for S1-QW is higher than p-InGaAs-QW. The QW peak positions are almost at the same energy in both samples. However, the broadening of the QW peak in the case of GaAs on sapphire is higher. This might be expected due to the higher interface roughness and/or higher defect density resulting from the mismatch in substrate and film material properties. Both can be improved and is the focus of our future work. While more research is required, we have presented the potential to realize an integrated microwave photonic chip on a sapphire platform.

# 4. Conclusion

We have investigated the effectiveness of LT GaAs layer on the quality of GaAs buffer on c-plane sapphire. The LT GaAs, at the early stage of growth, results in smooth surface morphology. The surface is

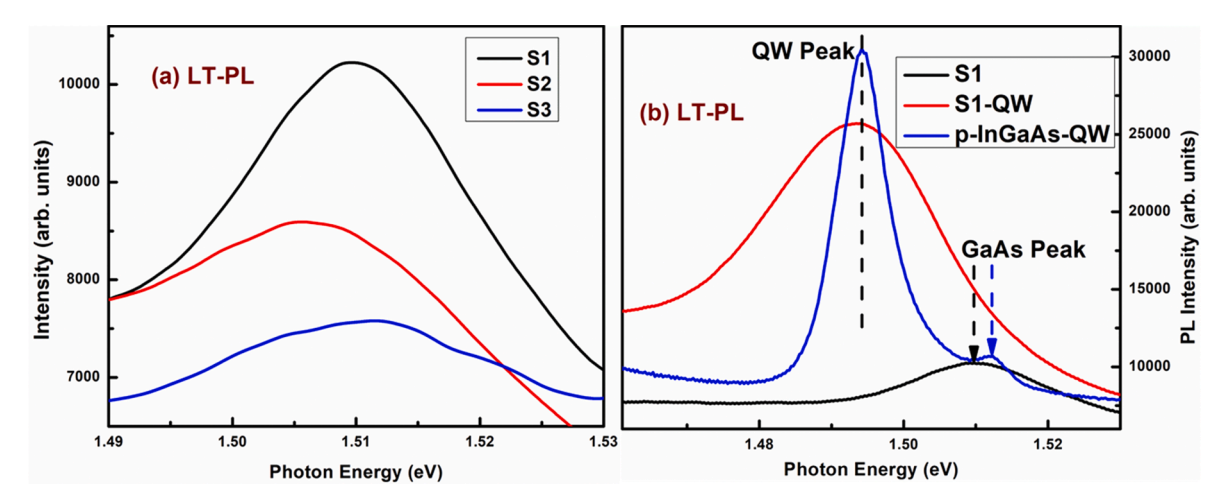


Fig. 7. (a) PL spectra of samples having three different thicknesses of LT layer and (b) PL of GaAs buffer (S1), InGaAs QW on sapphire (S1-QW), and InGaAs QW on GaAs substrate (p-InGaAs-QW). S1 PL repeated to show the shift of QW peak from GaAs, dashed arrow shows the GaAs PL peak position from homoepitaxial GaAs and GaAs on sapphire samples.

**Table 3**Integrated intensity, linewidth, and peak position of QW PL peak from both QW samples.

Sample ID	Integrated intensity (arb. units)	Linewidth (meV)	Peak position (meV)
S1-QW	550	32.53	1491.2
p-InGaAs- QW	192	9.12	1494.4

also described by pyramidal mounds and randomly shaped pits. The presence of pyramidal features is explained by high Ehrlich-Schwöbel (ES) barriers and adatom motion in the presence of stacking faults, while the pits are attributed to thermal etching by Ga droplets which form due to the lower sticking coefficient of arsenic on a GaAs (111)A surface. XRD omega-2theta scan and Raman results indicate that the absence of LT GaAs results in compressively strained GaAs which matches our speculation on the atomic arrangement. Phi-scan shows almost no twinning and HRTEM indicate an abrupt interface between film and substrate with very defects mostly confined near film/substrate interface. Rocking curves of these films can be fitted with two Gaussian showing the two different regions of different quality material which are also confirmed by HRTEM images. Together, these observations indicate that the GaAs buffer with the LT layer is effective in achieving highquality GaAs on sapphire and demonstrates the potential to realize an integrated microwave photonic chip on a sapphire platform although much work is needed to be done.

# CRediT authorship contribution statement

Rahul Kumar: Data curation, Methodology, Writing - original draft. Samir K. Saha: Investigation, Visualization. Andrian Kuchuk: Data curation, Formal analysis. Yurii Maidaniuk: Data curation. Fernando Maia de Oliveira: Data curation. Qigeng Yan: Data curation. Mourad Benamara: Data curation. Yuriy I. Mazur: Project administration. Shui-Qing Yu: Conceptualization, Funding acquisition. Gregory J. Salamo: Writing - review & editing, Conceptualization, Funding acquisition.

# Declaration of competing interest

The authors declare that they have no known competing financial interests or personal relationships that could have appeared to influence the work reported in this paper.

### Acknowledgment

The authors acknowledge the financial support by the Institute of Nanoscale Science and Engineering, University of Arkansas, and the Project "Quantum Interfaces of Dissimilar Materials" funded by National Science Foundation (NSF) (Grant No. 1809054). Additionally, Dr. Shui-Qing Yu would also like to acknowledge the NSF funding support ECCS1745143.

#### References

- P. Mukhopadhyay, R. Kumar, S. Ghosh, A. Chakraborty, A. Bag, S. Kabi, P. Banerji,
   D. Biswas, A novel growth strategy and characterization of fully relaxed un-tilted
   FCC GaAs on Si(100), J. Cryst. Growth 418 (2015) 138–144, https://doi.org/ 10.1016/j.jcrysgro.2015.02.030.
- [2] R. Kumar, Y. Maidaniuk, A. Kuchuk, S.K. Saha, P.K. Ghosh, Y.I. Mazur, M.E. Ware, G.J. Salamo, Excitation intensity and thickness dependent emission mechanism from an ultrathin InAs layer in GaAs matrix, J. Appl. Phys. 124 (2018), 235303, https://doi.org/10.1063/1.5053412.
- [3] S.K. Saha, R. Kumar, A. Kuchuk, H. Stanchu, Y.I. Mazur, S.Q. Yu, G.J. Salamo, GaAs epitaxial growth on R-plane sapphire substrate, J. Cryst. Growth 548 (2020), 125848, https://doi.org/10.1016/j.jcrysgro.2020.125848.
- [4] S.K. Saha, R. Kumar, A. Kuchuk, M.Z. Alavijeh, Y. Maidaniuk, Y.I. Mazur, S.Q. Yu, G.J. Salamo, Crystalline GaAs thin film growth on a c-plane sapphire substrate, Cryst. Growth Des. 19 (2019) 5088–5096, https://doi.org/10.1021/acs.cgd.9b00448.
- [5] T. Nakasu, T. Kizu, S. Yamashita, T. Aiba, S. Hattori, W.C. Sun, K. Taguri, F. Kazami, Y. Hashimoto, S. Ozaki, M. Kobayashi, T. Asahi, Surface texture and crystallinity variation of ZnTe epilayers grown on the step-terrace structure of the sapphire substrate, J. Electron. Mater. 45 (2016) 2127–2132, https://doi.org/10.1007/s11664-016-4386-8.
- [6] A. Sugimura, T. Hosoi, K. Ishibitsu, T. Kawamura, Heteroepitaxial growth of GaAs on sapphire substrates by a three-step method using low pressure MOCVD, J. Cryst. Growth 77 (1986) 524–529, https://doi.org/10.1016/0022-0248(86)90347-7.
- [7] K. Kasai, K. Nakai, M. Ozeki, Material and device properties of GaAs on sapphire grown by metalorganic chemical vapor deposition, J. Appl. Phys. 60 (1986) 1–5, https://doi.org/10.1063/1.337680.
- [8] T.P. Humphreys, C.J. Miner, J.B. Posthill, K. Das, M.K. Summerville, R. J. Nemanich, C.A. Sukow, N.R. Parikh, Heteroepitaxial growth and characterization of GaAs on silicon-on-sapphire and sapphire substrates, Appl. Phys. Lett. 54 (1989) 1687–1689, https://doi.org/10.1063/1.101303.
- [9] T.P. Humphreys, C.J. Miner, N.R. Parikh, K. Das, M.K. Summerville, J.B. Posthill, R.J. Nemanich, C.A. Sukow, Molecular beam epitaxial growth and characterization of GaAs on sapphire and silicon-on-sapphire substrates, MRS Proc. 144 (1988) 195, https://doi.org/10.1557/PROC-144-195.
- [10] T.F. Kuech, A. Segmüller, T.S. Kuan, M.S. Goorsky, Growth and properties of thin GaAs epitaxial layers on Al 2 O 3, J. Appl. Phys. 67 (1990) 6497–6506, https://doi. org/10.1063/1.345125.
- [11] L.C. Chuang, M. Moewe, K.W. Ng, T.-T.D. Tran, S. Crankshaw, R. Chen, W.S. Ko, C. Chang-Hasnain, GaAs nanoneedles grown on sapphire, Appl. Phys. Lett. 98 (2011), 123101, https://doi.org/10.1063/1.3567492.
- [12] L. Esposito, S. Bietti, A. Fedorov, R. Nötzel, S. Sanguinetti, Ehrlich-Schwöbel effect on the growth dynamics of GaAs(111)A surfaces, Phys, Rev. Mater. 1 (2017) 2–9, https://doi.org/10.1103/PhysRevMaterials.1.024602.

- [13] R. Kumar, P. Mukhopadhyay, a. Bag, S.K. Jana, a. Chakraborty, S. Das, M.K. Mahata, D. Biswas, Comparison of different pathways in metamorphic graded buffers on GaAs substrate: indium incorporation with surface roughness, Appl. Surf. Sci. 324 (2015) 304–309. doi:https://doi.org/10.1016/j.apsusc.2014.10.155.
- [14] R. Kumar, A. Bag, P. Mukhopadhyay, S. Das, D. Biswas, Comparison of different grading schemes in InGaAs metamorphic buffers on GaAs substrate: tilt dependence on cross-hatch irregularities, Appl. Surf. Sci. 357 (2015) 922–930, https://doi.org/10.1016/j.apsusc.2015.09.145.
- [15] H. Ehsani, I. Bhat, R.J. Gutmann, G. Charache, M. Freeman, Role of relative tilt on the structural properties of GalnSb epitaxial layers grown on (001) GaSb substrates, J. Appl. Phys. 86 (1999) 835, https://doi.org/10.1063/1.370811.
- [16] M.O. Petrushkov, M.A. Putyato, A.K. Gutakovsky, V.V. Preobrazhenskii, I. D. Loshkarev, E.A. Emelyanov, B.R. Semyagin, A.V. Vasev, Impact of LT-GaAs layers on crystalline properties of the epitaxial GaAs films grown by MBE on Si substrates, J. Phys. Conf. Ser. 741 (2016), https://doi.org/10.1088/1742-6596/741/1/012020.
- [17] D.S. Abramkin, M.O. Petrushkov, E.A. Emel'yanov, M.A. Putyato, B.R. Semyagin, A.V. Vasev, M.Y. Esin, I.D. Loshkarev, A.K. Gutakovskii, V.V. Preobrazhenskii, T. S. Shamirzaev, Influence of a low-temperature GaAs dislocation filter on the perfection of GaAs/Si layers, Optoelectron. Instrum. Data Process. 54 (2018) 181–186, https://doi.org/10.3103/S8756699018020103.
- [18] N. Gopalakrishnan, K. Baskar, H. Kawanami, I. Sakata, Effects of the low temperature grown buffer layer thickness on the growth of GaAs on Si by MBE, J. Cryst. Growth 250 (2003) 29–33, https://doi.org/10.1016/S0022-0248(02) 02210-8
- [19] S. Lee, Y.H. Im, Y.-B. Hahn, Two-step growth of ZnO films on silicon by atomic layer deposition, Korean J. Chem. Eng. 22 (2005) 334–338, https://doi.org/ 10.1007/BF02701506
- [20] C.C. Phua, T.C. Chong, W.S. Lau, Improved crystalline quality of molecular beam epitaxy grown GaAs-on-Si epilayer through the use of low-temperature gaas intermediate layer, Jpn. J. Appl. Phys. 33 (1994) L405–L408, https://doi.org/ 10.1143/JJAP.33.L405.
- [21] T.M. Burbaev, A.A. Gorbatsevich, V.I. Egorkin, I.P. Kazakov, V.P. Martovitskii, N. N. Mel'nik, Y.A. Mityagin, V.N. Murzin, S.A. Savinov, S.S. Shmelev, Comprehensive study of structural and optical properties of LT-GaAs epitaxial

- structures, Bull. Lebedev Phys. Inst. 40 (2013) 219–224, https://doi.org/10.3103/ \$1068335613080022.
- [22] J. Li, G. Miao, Z. Zhang, Y. Zeng, Experiments and analysis of the two-step growth of InGaAs on GaAs substrate, CrystEngComm. 17 (2015) 5808–5813, https://doi. org/10.1039/C5CE00979K.
- [23] Yu.B.Bolkhovityanov and O.P.Pchelyakov, GaAs epitaxy on Si substrates:modern status of research and engineering, Uspekhi Fiz. Nauk. 51 (2008) 437–456. doi: 10.3367/ufnr.0178.200805b.0459.
- [24] H.J. Kim, A. Duzik, S.H. Choi, Lattice-alignment mechanism of SiGe on sapphire, Acta Mater. 145 (2018) 1–7, https://doi.org/10.1016/j.actamat.2017.11.031.
- [25] Y. Horikoshi, T. Uehara, T. Iwai, I. Yoshiba, Area selective growth of GaAs by migration-enhanced epitaxy, Phys. Status Solidi Basic Res. 244 (2007) 2697–2706, https://doi.org/10.1002/pssb.200675621.
- [26] T. Uehara, T. Iwai, I. Yoshiba, Y. Horikoshi, Area-selective epitaxial growth of GaAs on GaAs(111)A substrates by migration-enhanced epitaxy, Jpn. J. Appl. Phys. 46 (2007) 496–501, https://doi.org/10.1143/JJAP.46.496.
- [27] M.S. Abrahams, C.J. Buiocchi, Etching of dislocations on the low-index faces of GaAs, J. Appl. Phys. 36 (1965) 2855–2863, https://doi.org/10.1063/1.1714594.
- [28] S. Kanjanachuchai, C. Euaruksakul, Self-running Ga droplets on GaAs (111)A and (111)B surfaces, ACS Appl. Mater. Interfaces 5 (2013) 7709–7713, https://doi.org/ 10.1021/am402455u
- [29] D. Zeng, W. Jie, T. Wang, J. Zhang, G. Zha, Type and formation mechanism of thermal etch pit on annealed (111) CdZnTe surface, Thin Solid Films 517 (2009) 2896–2899, https://doi.org/10.1016/J.TSF.2008.11.107.
- [30] H. Maki, T. Ikoma, I. Sakaguchi, N. Ohashi, H. Haneda, J. Tanaka, N. Ichinose, Control of surface morphology of ZnO (0001) by hydrochloric acid etching, Thin Solid Films 411 (2002) 91–95, https://doi.org/10.1016/S0040-6090(02)00194-3.
- [31] K. Sato, M.R. Fahy, B.A. Joyce, The growth of high quality GaAs on GaAs (111)A, Jpn. J. Appl. Phys. 33 (1994) L905–L907, https://doi.org/10.1143/JJAP.33.L905.
- [32] R. Kumar, D. Biswas, Tilt investigation of In(Al,Ga)As metamorphic buffer layers on GaAs (001) substrate: a novel technique for tilt determination, Cryst. Res. Technol. 51 (2016) 723–729, https://doi.org/10.1002/crat.201600149.
- [33] J.P. Bosco, G.M. Kimball, N.S. Lewis, H.A. Atwater, Pseudomorphic growth and strain relaxation of α-Zn3P2 on GaAs(001) by molecular beam epitaxy, J. Cryst. Growth 363 (2013) 205–210, https://doi.org/10.1016/J.JCRYSGRO.2012.10.054.